Published in final edited form as:
J Biol Chem. 2007 February 23; 282(8): 5296–5301. doi:10.1074/jbc.M609343200.

Fast and Selective Ammonia Transport by Aquaporin-8*

Sapar M. Saparov[‡], **Kun Liu**[§], **Peter Agre**[§], and **Peter Pohl**[‡,1]

[‡] Institut für Biophysik, Kepler Universität Linz, Altenbergerstrasse 69, A-4040 Linz, Austria

[§] Department of Cell Biology, Duke University Medical Center, Durham, North Carolina 27710

Abstract

The transport of ammonia/ammonium is fundamental to nitrogen metabolism in all forms of life. So far, no clear picture has emerged as to whether a protein channel is capable of transporting exclusively neutral NH_3 while excluding H^+ and NH_4^+. Our research is the first stoichiometric study to show the selective transport of NH_3 by a membrane channel. The purified water channel protein aquaporin-8 was reconstituted into planar bilayers, and the exclusion of NH_4^+ or H^+ was established by ensuring a lack of current under voltage clamp conditions. The single channel water permeability coefficient of 1.2×10^{-14} cm^3/subunit/s was established by imposing an osmotic gradient across reconstituted planar bilayers, and resulting minute changes in ionic concentration close to the membrane surface were detected. It is more than 2-fold smaller than the single channel ammonia permeability (2.7×10^{-14} cm^3/subunit/s) that was derived by establishing a transmembrane ammonium concentration gradient and measuring the resulting concentration increases adjacent to the membrane. This permeability ratio suggests that electrically silent ammonia transport may be the main function of AQP8.

Aquaporins (AQPs)[2] are commonly believed to mediate fast and selective water transport (1). However, some members of the protein family may have other functions. The intracellular acid-sensing aquaporin-6 (AQP6), for example, serves as an anion channel (2). The function of aquaporin-8 (AQP8) is under dispute. First, it was suggested that AQP8-mediated water transport may be particularly important for the rapid expansion of mitochondrial volume (3). In a contrasting study, it was concluded that the rapid volume equilibration in mitochondria in response to an osmotic gradient was due to its small size (high surface-to-volume ratio) rather than to AQP-mediated high membrane water permeability (4). Moreover, only mild phenotype differences between wild-type and AQP8-deficient mice were found (5).

*This work was supported by the Austrian Science Fund (FWF W1201-N13).

[1] To whom correspondence should be addressed. peter.pohl@jku.at. .

Publisher's Disclaimer: This work was supported by the Austrian Science Fund (FWF W1201-N13). The costs of publication of this article were defrayed in part by the payment of page charges. This article must therefore be hereby marked “advertisement” in accordance with 18 U.S.C. Section 1734 solely to indicate this fact.

[2]The abbreviations used are:

AQP aquaporin

MES 4-morpholineethanesulfonic acid

MOPS4-morpholinepropanesulfonic acid.

Europe PMC Funders Author Manuscripts

In addition, AQP8 was anticipated to participate in ammonia transport. AQP8 was able to rescue the growth of yeast defective in ammonium uptake, suggesting that the protein is involved in NH_3 transport in humans. Increased acidification of the oocyte medium containing NH_4^+ was in accordance with NH_3 diffusion through the protein (6). Voltage clamp experiments suggested that AQP8 conducts NH_4^+ as well (7). Because growth complementation could be an indirect effect of AQP8 expression, light-scattering experiments with reconstituted vesicles were conducted. They revealed AQP8 permeability to formamide, suggesting that the protein may transport ammonium *in vivo* and physiologically contribute to the acid-base equilibrium (8). However, comparative phenotype studies in wild-type *versus* AQP8 null mice revealed no significant or only very small differences in serum ammonia, colonic ammonia absorption, renal ammonia clearance, and liver ammonia accumulation (9). It is difficult to interpret these results as evidence against physiologically significant AQP8-facilitated NH_3 transport in mice. Because of the importance of ammonium homeostasis, several ammonium transport pathways are likely to exist. This is crucial for the urine pH adjustment and the acid-base equilibrium of body fluid. One of the alternative NH_3 transport pathways was identified in terms of RhBG and RhCG, the non-erythroid members of the Rh family (10). These proteins were also knocked out in mice, and neither distal tubular acidosis nor hyperammonemia was detected (11).

The assumption that a double knock out of both AQP8 and Rh proteins leads to a detectable phenotype remains to be tested. This expectation is based on the observation that the apical membranes of AQP8-expressing cells must maintain large chemical and osmotic gradients and therefore be effectively impermeable to small molecules, including NH_3 and water. Tightening of the lipid matrix and, thus, a reduced permeability is achieved by high concentrations of glycosphingolipids and sphingomyelin in the outer membrane leaflet (12). It is therefore not surprising that, for example, the expression of hepatic AQP8 was associated with apical microdomain fractions enriched in cholesterol and sphingolipids (13). With respect to the low basal NH_3 permeability of the epithelial membrane, the requirement for controllable proteinaceous NH_3 transport machinery becomes obvious. AQP8 is the ideal candidate because it is largely localized in intracellular vesicles and can be redistributed to plasma membranes via a microtubule-dependent, cAMP-stimulated mechanism (14).

The molecular mechanism for ammonia transport by AQP8 has not yet been resolved. Evidence was reported showing both NH_3 and NH_4^+ transport (7), although it was not possible to differentiate whether NH_4^+ transport occurred through the aquaporin itself or whether secondary effects related to rapid NH_3 transport took place. We have addressed this question by reconstituting purified AQP8 into planar lipid bilayers mimicking the lipid composition of epithelial plasma membranes. Functional reconstitution was confirmed by water flux measurements. Simultaneous ion and ammonia flux measurements revealed perfect NH_3 selectivity, *i.e.* ammonia transport by AQP8 is electrically silent. We found that ammonia permeability exceeds water permeability 2-fold, suggesting that ammonia transport may be the main function of AQP8.

EXPERIMENTAL PROCEDURES

Expression and Purification of AQP8 from Yeast

Rat AQP8 was expressed in *pep4*Δ *Saccharomyces cerevisiae* and purified as previously described (8). In brief, after induction with 2% (w/w) galactose harvested by centrifugation, and three French press cycles, the membrane fraction was recovered from the supernatant by ultracentrifugation. AQP8 protein was solubilized in *n*-octyl-β-D-glucoside. The His_{10}-tagged protein was absorbed by a nickel column. Its purity was better than 90% as revealed by the comparison of Coomassie-stained SDS gels with bands obtained by immunoblotting.

Protein Reconstitution into Planar Bilayers

Purified AQP8 proteins were first reconstituted into proteoliposomes by dialysis (15). In brief, the reconstitution mixture was prepared at room temperature by sequentially adding 100 mM MOPS-sodium, pH 7.5 (Fluka, Buchs, Switzerland), 1.25% (w/v) octyl glucoside, purified AQP8 (final concentration 0.5–1 mg/ml), and 20–50 mg/ml of preformed lipid vesicles. The latter consisted of a 3:2:1 molar mixture of cholesterol, *E. coli* lipid extract (Avanti Polar Lipids, Alabaster, AL), and sphingomyelin. It was loaded into SPECTRA/POR 2.1 dialysis tubing, molecular weight cut-off 15,000 (Spectrum Laboratories, Laguna Hills, CA), and dialyzed against 100 volumes of assay buffer for 48 h at 4 °C. Proteoliposomes were harvested by ultracentrifugation (60 min at 100,000 × *g*) and were resuspended into assay buffer (compare Fig. 1) at a concentration of 5–10 mg/ml.

At the air-water interface of vesicle suspensions, monolayers were formed spontaneously (16). Two such monolayers were combined to form a planar bilayer in the 150-μm-diameter aperture of a 25-μm-thick polytetrafluoroethylene septum separating the two aqueous phases of the chamber (15, 17). The septum was pretreated with a hexadecane-hexane mixture (volume ratio of 1:200).

Water Flux Measurements

Transmembrane osmotic water flow was derived from solute dilution in the immediate membrane vicinity (18). The solute concentration at the interface, C_s, increases with the distance, x, to the membrane: $C(x) = C_s\exp(-vx/D+bx^3/3D)$, where $-v$ and b are – the linear drift velocity of the osmotic volume flow and the stirring parameter, respectively. In the steady state, v was obtained by fitting the concentration distribution of Na^+ ions to this equation. v is related to P_f by $P_f=v/(C_{osm}\ V_w)$ (19). J_w is the product of water concentration and v. Na^+ concentrations were measured by microelectrodes made of glass capillaries, the tips (1–2 μm in diameter) of which were filled with mixture A of Sodium Ionophore I (Fluka, Dreisenhofen, Germany). Movement of the electrodes relative to the membrane was realized by a hydraulic stepdrive (Narishige).

Ion Flux Measurements

Ag/AgCl reference electrodes were immersed into the buffer solutions at both sides of the planar bilayers. Under voltage clamp conditions, the transmembrane current was measured by a patch clamp amplifier (model EPC9; HEKA Electronics). The recording filter was a 4-pole Bessel with 3-dB corner frequency of 0.1 kHz. The acquired raw data were analyzed with the help of the TAC software package (Bruxton Corp., Seattle, WA). A Gaussian filter of 0.3 Hz was applied to reduce noise.

Ammonia Flux Measurements

Ammonium chloride was added to the buffer solutions surrounding the bilayer. Its concentration at the *cis* side of the membrane was higher than at the *trans* side. The resulting transmembrane NH_3 flux gave rise to a pH and a NH_4^+ gradient in the immediate membrane vicinity. The latter was measured in terms of a potential difference between a selective microelectrode and a reference electrode, both placed in the buffer solution at the same side of the membrane (20). Movement of the electrodes relative to the membrane was realized by a hydraulic stepdrive (Narishige).

Theoretical Model for NH_3 Transport

In the model, the membrane flux of NH_4^+ is neglected. This assumption is justified by the lack of any incremental conductivity after AQP8 reconstitution (Fig. 2). For acidic pH the experimental results are analyzed precisely by solving the complete system of differential

equations that takes into account all relevant chemical reactions in the immediate membrane vicinity (20, 21) as shown in Equations 1 and 2.

$$J_i = -D_i dc_i/dx_i, \quad i=1,\ldots,6 \quad \text{(Eq. 1)}$$

$$dJ_i/dx = R_i(c), \quad c=(c_1,\ldots,c_6) \quad \text{(Eq. 2)}$$

J_i, D_i, $c_i(x)$ denote, respectively, flux, diffusion coefficient, and concentration of the ith species, where 1 = H^+, 2 = NH_3, 3=NH_4^+, 4 = OH^-, 5 = MES^-, 6 = H-MES. $R_i(c)$ is the specific local rate of expenditure of the ith species in chemical reactions 1 and 2.

$$H^+ + NH_3 \leftrightarrows NH_4^+; \quad H^+ + OH^- \leftrightarrows H_2O \quad \text{REACTION 1}$$

$$H^+ + MES^- \leftrightarrows H{-}MES \quad \text{REACTION 2}$$

At the membrane-water interface, the fluxes of all species are required to be equal to zero, except for J_2, as shown in Equation 3.

$$J_1 = J_3 = J_4 = \ldots = J_8 = 0; \quad J_2 = J \quad \text{(Eq. 3)}$$

For other boundary conditions, please compare Antonenko *et al.* (21). The numerical solutions are derived, assuming that the rates of chemical reactions (like dissociation/recombination of water, buffer, and NH_3) are very high compared with the rate of diffusion through the USL, so that the local chemical equilibrium is maintained.

RESULTS

To demonstrate functional reconstitution, we measured osmotic water flow through purified AQP8 channels by imposing an osmotic gradient across reconstituted planar bilayers and detected resulting minute changes in ionic concentration close to the membrane surface (15, 17). We formed planar membranes that mimicked the composition of epithelial cells (cholesterol:*E. coli* lipid extract:sphingomyelin = 3:2:1). In line with previous experiments (12), these membranes exhibited a very low osmotic water permeability, P_f, of only (11.0 ± 1.5) μm/s. Reconstitution of AQP8 at lipid:protein mass ratio, r_m = 100, resulted in a 3-fold increase in P_f (Fig. 1). The incremental water permeability, $P_{f,c}$, allowed calculation of the hydraulic permeability coefficient of a single channel, p_f, from the absolute hydraulic conductivity of all channels $P_{f,c}$ and the number of channels, n (19). n is anticipated to be equal to the total number of lipid molecules, L, in the bilayer divided by the molar lipid to protein ratio, r, where L is derived from two times (for both leaflets) the membrane area, A, divided by the area, b, per lipid molecule as shown in Equation 4

$$P_f = P_{f,c} A/n = P_{f,c} Ar/2L = P_{f,c} br_m M_p/2M_L \quad \text{(Eq. 4)}$$

where M_P and M_L are the molecular masses of the protein (30 kDa) and the lipid (700 Da), respectively. For b = 70 A^2, p_f of AQP8 is found to be (2.4 ± 0.2) × 10^{-14} cm^3 $subunit^{-1}$ s^{-1}. The result was obtained assuming that protein incorporation is 100% efficient. The real efficiency is, most probably, smaller. Reconstitution of AQP0, for example, was ~50% efficient (22). If our value is in the same range, p_f adopts a value of ~(1.2 ± 0.1) × 10^{-14} cm^3 $subunit^{-1}$ s^{-1}. That is in reasonable agreement with results reported previously using a *Xenopus* oocyte expression system (23). p_f allows calculation of the AQP8 turnover numbers for water, T_W as shown in Equation 5

$$T_w = N_A p_f / V_w = 4 \cdot 10^8\ s^{-1} \quad \text{(Eq. 5)}$$

where N_A and V_W are the Avogadro number and the molecular volume of water, respectively.

Demonstration of functional reconstitution was followed by probing NH_4^+ transport through AQP8. A hundredfold augmentation of the NH_4Cl bulk concentration did not alter the current voltage characteristics of bare lipid bilayers or membranes reconstituted with AQP8 (Fig. 2). The similarity of ion conductivities indicated that AQP8 excluded NH_4^+ ions. Even if the entire conductivity of G = 5 nS cm^{-2} were attributed to the protein, the total ion flux, j_{ion}, did not exceed 10^{-15} mol cm^{-2} s^{-1} as calculated according to Equation 6.

$$j_{ion} = \frac{RT}{z^2 F^2} G \quad \text{(Eq. 6)}$$

Consequently, the ion:water selectivity was better than $1:10^9$ (compare Refs. 17, 24).

Subsequently, transport of neutral NH_3 molecules by AQP8 was tested. At acidic pH, a transmembrane NH_3 flux, $J^M_{NH_3}$, was expected to give rise to a NH_4^+ flux through the near-membrane aqueous stagnant layers (20) as shown in Equations 7 and 8.

$$J^M_{NH_3} = -D_{NH_3} \frac{d[NH_3]}{dx} - D_{NH_4^+} \frac{d\left[NH_4^+\right]}{dx} \quad \text{(Eq. 7)}$$

$$J^M_{NH_3} = -D_{NH_4^+} \frac{d\left[NH_4^+\right]}{dx} (1+\alpha) \quad \text{(Eq. 8)}$$

D_{NH_3}, $D_{NH_4^+}$, and x are the aqueous diffusion coefficients of NH_3, NH_4^+, and the distance to the membrane, respectively. α is equal to $10^{(pH - pK)}$. A NH_4^+ concentration gradient was imposed across the planar bilayer, and the resulting small changes in NH_4^+ concentration close to the membrane were detected by scanning ammonia-selective microelectrodes. The difference in NH_4^+ polarization adjacent to bare (Fig. 3*A*) and reconstituted planar bilayers (Fig. 3*B*) indicated NH_3 transport by aquaporins. Plotting $J^M_{NH_3}$ *versus* the NH_4^+ transmembrane concentration gradient reveals a linear dependence (Fig. 3*C*). Calculation of $J^M_{NH_3}$ was performed taking into account the accompanying chemical reactions of ammonia and buffer. The set of differential equations (see “Experimental Procedures”) was solved numerically to fit the experimental profiles for 0 < X < 50 μm (20, 21). NH_3 permeabilities of 16 and 105 μm/s were computed for bare and AQP8-containing bilayers, respectively.

Protein inhibition by Hg^{2+} was testable, although the ammonia-selective microelectrode was less sensitive in the presence of Hg^{2+} (a 10-fold change in NH_4^+ concentration corresponded to a change in microelectrode potential of only 27 mV instead of the usually measured 52 mV). In the particular experiment shown in Fig. 4, Hg^{2+} reduced the transmembrane NH_3 flux from 0.2 to 0.06 nmol cm^{-2} s^{-1}. Thus, the NH_3 permeability of the planar bilayer reconstituted with AQP8 decreased from 50 to 15 μm/s, indicating complete AQP8 inhibition.

Europe PMC Funders Author Manuscripts

For further proof of NH_3 conductance by AQP8, flux dependence on membrane protein abundance was measured. Reconstitution of increasing amounts of AQP8 was accompanied by an increasing NH_4^+ concentration polarization in the immediate membrane vicinity (Fig. 5). As before, the set of differential equations (see "Experimental Procedures") was solved numerically for different $P^M_{NH_3}$. For each parameter AQP8 concentration the parameter was changed iteratively until the deviation of the theoretical profile from the experimental one was minimal. Plotting $P^M_{NH_3}$ as a function of $1/r_m$ allowed calculation of single channel ammonium permeability (Fig. 5, *inset*) as shown in Equation 9

$$p_{NH_3} = P_{NH_{3,c}} A/n = P_{NH_{3,c}} br_m M_p / 2M_L \quad \text{(Eq. 9)}$$

where $P_{NH_{3,c}}$ is the incremental NH_3 permeability introduced by AQP8 reconstitution. Assuming 50% reconstitution efficiency p_{NH_3} was equal to $(2.7 \pm 0.2) \times 10^{-14}$ cm^3 $subunit^{-1}$ s^{-1} and, thus, 2-fold higher than the respective single channel coefficient for water. The number of neutral ammonia molecules, T_{NH_3}, transported by AQP8 per second can be assessed by calculation of the turnover number per channel as shown in Equation 10

$$T_{NH_3} = N_A p_{NH_3} / V_{NH_3} = 7.7 \cdot 10^5 \ s^{-1} \quad \text{(Eq. 10)}$$

where N_A and V_{NH_3} are the Avogadro number and the molecular volume of NH_3, respectively.

DISCUSSION

We have shown that AQP8 transports both water and ammonia very efficiently. Reconstitution of the purified protein increased the respective permeabilities of model membranes mimicking apical membranes of epithelial cells up to 3- or 6-fold. As most members of the aquaporin family (25, 26), AQP8 prevents ions from passing the channel, *i.e.* it allows exclusive transport of the neutral NH_3 molecule. This observation contrasts with the proposed NH_4^+ permeability of AQP8 made in the *Xenopus* oocyte expression system (7). However, the ion fluxes detected in the oocyte system are not necessarily NH_4^+ fluxes. They may also represent endogenous pH-sensitive currents of the oocyte. Because NH_3 acidifies the aqueous solution it leaves behind and augments the pH in the solution it enters (20), a transmembrane proton gradient builds up that gives rise to proton and counterion currents, provided that the membrane is permeable to these charged species. Subtracting the membrane permeability of non-transfected oocytes may be misleading because the expression of integral membrane proteins may modify ion channels endogenous to *Xenopus* oocytes (27). Because reconstituted planar bilayers lack these disadvantages and because their extremely low intrinsic proton (24) and ion permeabilities (15, 17) are not altered by AQP8, it is concluded that the protein excludes NH_4^+.

AQP8 transports ammonia very efficiently. With ~8×10^5 substrate molecules/s/channel (Equation 10), T_{NH_3} of AQP8 is comparable with the respective number of 2×10^6 estimated for the human rhesus-associated glycoprotein (28). Because the physiological NH_3 concentration is orders of magnitude smaller than the concentration of H_2O, the NH_3 conduction rate need not be as high as that of H_2O to match diffusion limited rates for arriving at the pore (29). In agreement with this prediction, we have obtained a 500-fold higher T_W (Equation 5).

Comparison of the actual single channel permeability coefficients reveals, in contrast, a preference for NH_3 over H_2O as shown in Equation 11.

$$p_f/p_{NH_3} = 1.2/2.7 \cong 1/2 \quad \text{(Eq. 11)}$$

Because of their larger molecular volume ($V_{NH_3} \gg V_W$), the channel accommodates less gas than water molecules. Thus, albeit their higher transport velocity, AQP8 transports less NH_3 molecules than water molecules. It should be noted that the actual velocity of water transport may be underestimated because it was derived assuming that the pores are densely packed with water. In single file transport, the density of water inside the channel may be lower than in bulk (30, 31). Molecular dynamics simulations support the view that liquid-vapor oscillations occur in the channel (32, 33).

Equation 11 reveals a preference for ammonia over water. This result conflicts with a cell culture study in which the fluorescence of the pH-sensing yellow fluorescent protein was used to assess rat or mouse AQP8 ammonia permeability. The reason for the reported extremely low AQP8 single channel NH_3-to-water permeability of only 0.03 (9) is not clear. However, it is likely that the kinetics of pH changes are, at least in part, determined by compensatory transport events aimed to maintain cellular pH. Calculating P_{NH_3} from the time course of pH changes alone (9) should be hampered (i) by passive fluxes of CO_2 and H^+ through the plasma membrane as well as (ii) by different types of pH-regulating transporters, like cation-H^+ exchangers, HCO_3^- transporters, and H^+-ATPases, and (iii) proton exchange with intracellular compartments such as mitochondria and lysosomes. Lacking the entire list of uncertainties, reconstituted bilayers offer the opportunity to measure NH_3 flux directly. The only uncertainty of the bilayer system is that the reconstituted protein may adopt a slightly different quaternary structure. At least for the aqueous pore of the AQP8 monomer, which is the channel path for water and ammonia, this can be ruled out by the perfect match between the p_f values of the reconstituted protein and the one in an expression system (23). Theoretically, there is still a possibility that transport of charged species occurs through a putative fifth pore in the center of the aquaporin tetramer. It is rather unlikely in AQP8 because (i) so far ion channel activity has been ascribed only to AQP1 (34), (ii) nonphysiologically high cGMP concentrations (1 mM) are required (35), and (iii) ion channel activity was not reproduced by a variety of laboratories (36, 37).

AQP8 is the first ammonia-transporting channel for which the exclusion of NH_4^+ has been shown. The net transport of NH_3 across the plasma membrane by kidney Rh glycoproteins RhBG and RhCG results from an exchange of NH_4^+ for H^+ (38). A similar mechanism for AQP8 can be ruled out because the estimated upper limit of NH_4^+ or H^+ fluxes of 1×10^{-15} mol cm^{-2} s^{-1} is negligible compared with the ammonia flux of ~0.4 nmol cm^{-2} s^{-1} (Equation 6). NH_3/H^+ cotransport or NH_4^+ transport as proposed for AMT-1 from the hyperthermophilic archaeon *Archaeglobus fulgidus* (39) or the plant ammonium transporters LeAMT1 (40) and LeAMT2 (41) can be excluded for the same reason. Exclusion of NH_3 as well as saturable transport kinetics found for LeAMT1;1 (42) indicate a transporting mechanism that contrasts with AQP8.

A transport mechanism much closer to AQP8 has been proposed for AmtB from *E. coli.* Mainly based on structural considerations (43, 44) and on molecular dynamics simulations (45), NH_3 selectivity was suggested. However, occasional passage of NH_4^+ or H^+ was not excluded. It would be stabilized by ring currents of the rich aromatic environment at the constriction zone using the acid/base properties of the imidazole nitrogens to assist in proton transfer (43). The authors concluded that a stoichiometric measure of conductance of neutral and charged species is required to establish whether ion conductance takes place, a study we now have carried out for AQP8.

Summarizing, AQP8 exhibits a preference for neutral NH_3 molecules over water, suggesting a physiological role in maintenance of acid-base equilibrium. In physiological concentrations AQP8 may augment the basal NH_3 conductivity 3- to 5-fold.

Acknowledgments

We thank Quentina Beatty for critically reading the manuscript.

REFERENCES

1. King LS, Kozono D, Agre P. Nat. Rev. Mol. Cell Biol. 2004; 5:687–698. [PubMed: 15340377]
2. Yasui M, Hazama A, Kwon TH, Nielsen S, Guggino WB, Agre P. Nature. 1999; 402:184–187. [PubMed: 10647010]
3. Calamita G, Ferri D, Gena P, Liquori GE, Cavalier A, Thomas D, Svelto M. J. Biol. Chem. 2005; 280:17149–17153. [PubMed: 15749715]
4. Yang B, Zhao D, Verkman AS. J. Biol. Chem. 2006; 281:16202–16206. [PubMed: 16624821]
5. Yang B, Song Y, Zhao D, Verkman AS. Am. J. Physiol. 2005; 288:C1161–C1170.
6. Jahn TP, Moller ALB, Zeuthen T, Holm LM, Klaerke DA, Mohsin B, Kuhlbrandt W, Schjoerring JK. FEBS Lett. 2004; 574:31–36. [PubMed: 15358535]
7. Holm LM, Jahn TP, Moller AL, Schjoerring JK, Ferri D, Klaerke DA, Zeuthen T. Pflugers Arch. Eur. J. Physiol. 2005; 450:415–428. [PubMed: 15988592]
8. Liu K, Nagase H, Huang CG, Calamita G, Agre P. Biol. Cell. 2006; 98:153–161. [PubMed: 15948717]
9. Yang B, Zhao D, Solenov E, Verkman AS. Am. J. Physiol. 2006; 291:C417–C423.
10. Nakhoul NL, Dejong H, Abdulnour-Nakhoul SM, Boulpaep EL, Hering-Smith K, Hamm LL. Am. J. Physiol. 2005; 288:F170–F181.
11. Chambrey R, Goossens D, Quentin F, Eladari D. Transfus. Clin. Biol. 2006; 13:154–158. [PubMed: 16563831]
12. Krylov AV, Pohl P, Zeidel ML, Hill WG. J. Gen. Physiol. 2001; 118:333–340. [PubMed: 11585847]
13. Mazzone A, Tietz P, Jefferson J, Pagano R, Larusso NF. Hepatology. 2006; 43:287–296. [PubMed: 16440338]
14. Garcia F, Kierbel A, Larocca MC, Gradilone SA, Splinter P, La-Russo NF, Marinelli RA. J. Biol. Chem. 2001; 276:12147–12152. [PubMed: 11278499]
15. Saparov SM, Kozono D, Rothe U, Agre P, Pohl P. J. Biol. Chem. 2001; 276:31515–31520. [PubMed: 11410596]
16. Montal M, Darszon A, Schindler H. Q. Rev. Biophys. 1981; 14:1–79. [PubMed: 6269143]
17. Pohl P, Saparov SM, Borgnia MJ, Agre P. Proc. Natl. Acad. Sci. U. S. A. 2001; 98:9624–9629. [PubMed: 11493683]
18. Pohl P, Saparov SM, Antonenko YN. Biophys. J. 1997; 72:1711–1718. [PubMed: 9083675]
19. Finkelstein, A. Water Movement through Lipid Bilayers, Pores, and Plasma Membranes. Wiley & Sons; New York: 1987. p. 10-41.
20. Antonenko YN, Pohl P, Denisov GA. Biophys. J. 1997; 72:2187–2195. [PubMed: 9129821]
21. Antonenko YN, Denisov GA, Pohl P. Biophys. J. 1993; 64:1701–1710. [PubMed: 8369403]
22. Zampighi GA, Hall JE, Kreman M. Proc. Natl. Acad. Sci. U. S. A. 1985; 82:8468–8472. [PubMed: 2417221]
23. Ma T, Yang B, Verkman AS. Biochem. Biophys. Res. Commun. 1997; 240:324–328. [PubMed: 9388476]
24. Saparov SM, Tsunoda SP, Pohl P. Biol. Cell. 2005; 97:545–550. [PubMed: 15850456]
25. Nielsen S, Frokiaer J, Marples D, Kwon TH, Agre P, Knepper MA. Physiol. Rev. 2002; 82:205–244. [PubMed: 11773613]
26. Pohl P. Biol. Chem. 2004; 385:921–926. [PubMed: 15551866]

27. Shimbo K, Brassard DL, Lamb RA, Pinto LH. Biophys. J. 1995; 69:1819–1829. [PubMed: 8580325]
28. Ripoche P, Bertrand O, Gane P, Birkennmeier C, Colin Y, Cartron JP. Proc. Natl. Acad. Sci. U. S. A. 2004; 101:17222–17227. [PubMed: 15572441]
29. Winkler FK. Pflugers. Arch. Eur. J. Physiol. 2006; 451:701–707. [PubMed: 16273393]
30. Saparov SM, Pohl P. Proc. Natl. Acad. Sci. U. S. A. 2004; 101:4805–4809. [PubMed: 15034178]
31. Saparov SM, Pfeifer JR, Al-Momani L, Portella G, de Groot BL, Koert U, Pohl P. Phys. Rev. Lett. 2006; 96:148101. [PubMed: 16712124]
32. Beckstein O, Sansom MS. Proc. Natl. Acad. Sci. U. S. A. 2003; 100:7063–7068. [PubMed: 12740433]
33. Hummer G, Rasaiah JC, Noworyta JP. Nature. 2001; 414:188–190. [PubMed: 11700553]
34. Yool AJ, Weinstein AM. News Physiol. Sci. 2002; 17:68–72. [PubMed: 11909995]
35. Boassa D, Stamer WD, Yool AJ. J. Neurosci. 2006; 26:7811–7819. [PubMed: 16870726]
36. Agre P, Lee MD, Devidas S, Guggino WB, Sasaki S, Uchida S, Kuwahara M, Fushimi K, Marumo F, Verkman AS, Yang B, Deen PMT, Mulders SM, Kansen SM, van Os CH. Science. 1997; 275:1490–1492. [PubMed: 9045617]
37. Tsunoda SP, Wiesner B, Lorenz D, Rosenthal W, Pohl P. J. Biol. Chem. 2004; 279:11364–11367. [PubMed: 14701836]
38. Mak D-OD, Dang B, Weiner ID, Foskett JK, Westhoff CM. Am. J. Physiol. 2006; 290:F297–F305.
39. Andrade SL, Dickmanns A, Ficner R, Einsle O. Proc. Natl. Acad. Sci. U. S. A. 2005; 102:14994–14999. [PubMed: 16214888]
40. Ludewig U, von Wiren N, Frommer WB. J. Biol. Chem. 2002; 277:13548–13555. [PubMed: 11821433]
41. Mayer M, Schaaf G, Mouro I, Lopez C, Colin Y, Neumann P, Cartron JP, Ludewig U. J. Gen. Physiol. 2006; 127:133–144. [PubMed: 16446503]
42. Mayer M, Dynowski M, Ludewig U. Biochem. J. 2006; 396:431–437. [PubMed: 16499477]
43. Khademi S, O'Connell J III, Remis J, Robles-Colmenares Y, Miercke LJ, Stroud RM. Science. 2004; 305:1587–1594. [PubMed: 15361618]
44. Zheng L, Kostrewa D, Berneche S, Winkler FK, Li XD. Proc. Natl. Acad. Sci. U. S. A. 2004; 101:17090–17095. [PubMed: 15563598]
45. Lin Y, Cao Z, Mo Y. J. Am. Chem. Soc. 2006; 128:10876–10884. [PubMed: 16910683]

Europe PMC Funders Author Manuscripts

Europe PMC Funders Author Manuscripts

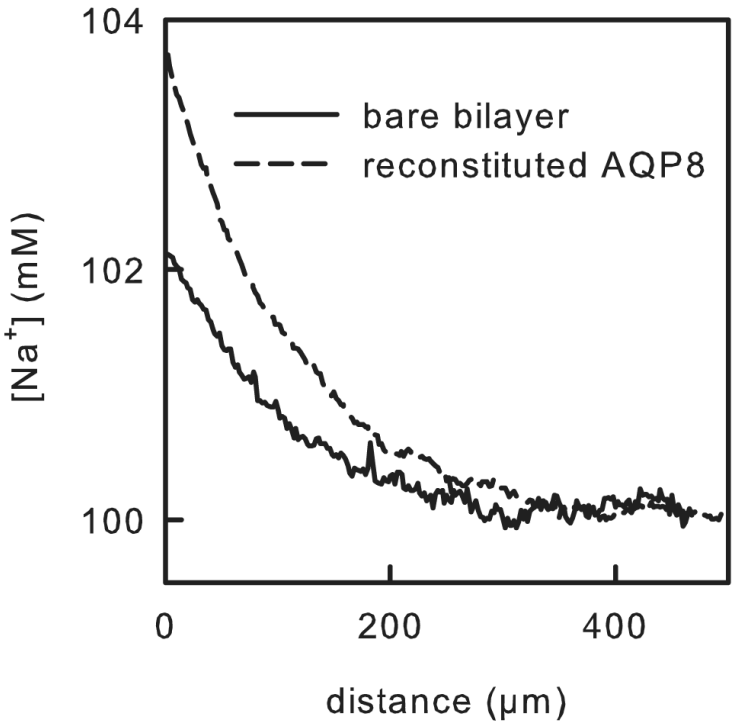

FIGURE 1. Water transport by AQP8

Reconstitution of AQP8 (protein:lipid = 1:100) augmented water permeability of bare lipid bilayers (cholesterol:*E. coli* lipid extract:sphingomyelin = 3:2:1) from 11 to 27 μm/s. Water permeability was calculated from the dilution of Na^+ ions shown as a function of the distance to the membrane. Osmotic water flux was induced by 1 M urea. The buffer contained 20 mM MES, 100 mM NaCl, 1 mM NH_4Cl, pH 6.0.

Europe PMC Funders Author Manuscripts

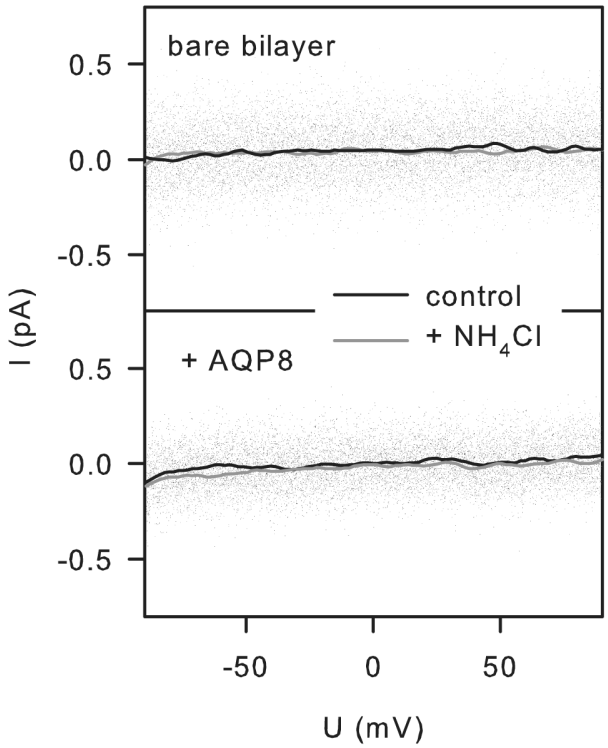

FIGURE 2. Exclusion of NH_4^+ transport by AQP8

The current voltage characteristics of bare lipid bilayers and bilayers reconstituted with AQP8 are not altered by the hundredfold augmentation of the NH_4Cl bulk concentration. A voltage ramp (duration 3 min) was applied in the interval from −90 to +90 mV. The current was measured with a frequency of 100 Hz and than filtered at 0.3 Hz (compare "Experimental Procedures"). The resulting data cloud is plotted. The *spline lines* were obtained by applying a local smoothing technique (100 intervals) using polynomial regression and weights computed from the Gaussian density function (SigmaPlot). The similarity of their slopes indicates that AQP8 excludes other ions as well. Membrane and buffer composition were as in Fig. 1.

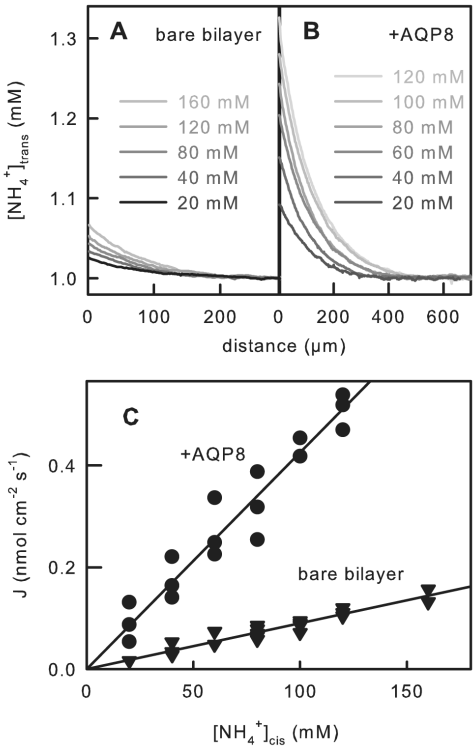

FIGURE 3. NH_3 flux *J* as a function of the transmembrane NH_4Cl concentration gradient

The NH_4^+ concentration in the *trans* compartment was measured by scanning microelectrodes as a function of the distance to the membrane. *A*, representative concentration profiles visualizing NH_3 diffusion through a bare lipid bilayer made of a lipid mixture (cholesterol:*E. coli* lipid extract:sphingomyelin = 3:2:1). *B*, representative concentration profiles showing NH_3 diffusion through reconstituted AQP8. For membrane formation the same lipid composition as in *panel A* was used. The protein:lipid ratio was 1:50. *C*, NH_3 flux at different NH_4^+ bulk concentrations in the *cis* compartment. J_{NH_3} and P_{NH_3} were calculated using the analytical model of weak base diffusion (Equations 1-3 and Reactions 1 and 2). The regression lines correspond to NH_3 permeabilities of 16 and 105 μm/s for bare and AQP8-containing bilayers, respectively. The buffer solution contained 20 mM MES, 100 mM NaCl, pH 6.0. The *trans* compartment contained 1 mM NH_4Cl.

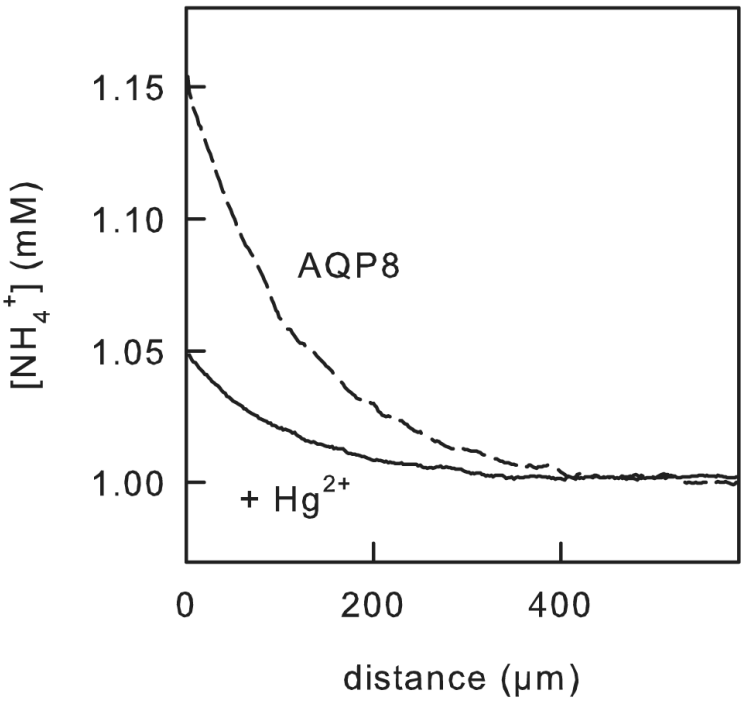

FIGURE 4. Inhibition of AQP8 mediated NH_3 transport by Hg^{2+}

Reconstitution of AQP8 in a protein:lipid ratio of 1:120 resulted in a NH_3 permeability of 50μm/s. 1 m$_M$ Hg^{2+} reduced the permeability to that of a bare bilayer (here to 15 μm/s). The corresponding transmembrane NH_3 fluxes were 0.2 and 0.06 nmol cm^{-2} s^{-1} in the absence and presence of Hg^{2+}, respectively. The *trans* and *cis* NH_4Cl concentrations in the bulk were equal to 1 and 80 m$_M$, respectively. Buffer composition was as in Fig. 1.

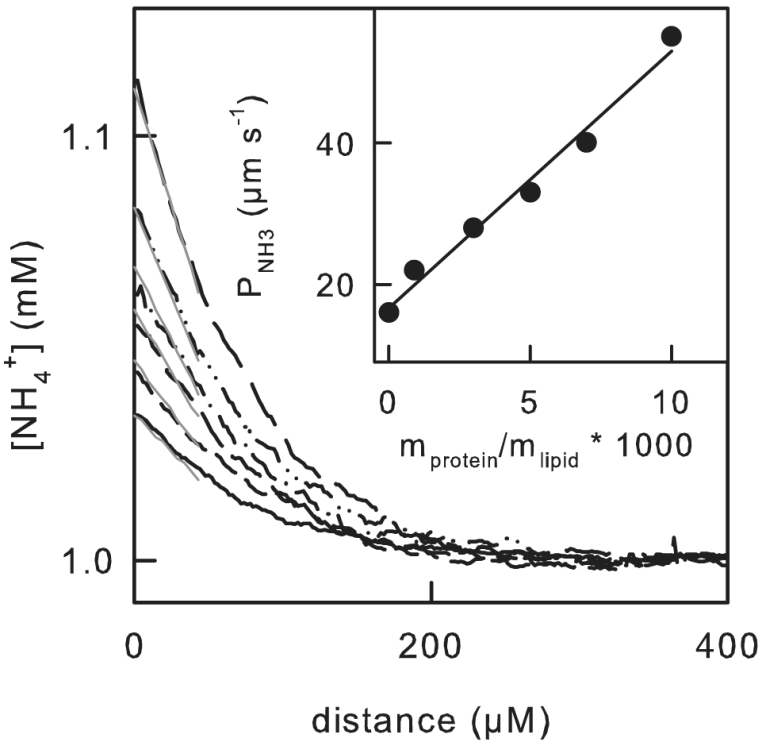

FIGURE 5. NH_3 membrane permeablity as a function of AQP8 membrane abundance

The *trans* and *cis* NH_4Cl concentrations in the bulk were equal to 1 and 80 mM, respectively. In the absence of the protein (*spline line*), a modest increase in the *cis* NH_4^+ concentration was observed in the immediate membrane vicinity. Upon reconstitution of AQP8, the augmentation of NH_4^+ concentration adjacent to the membrane became more pronounced. The more protein was reconstituted, the higher was the concentration polarization. The *gray lines* represent concentration profiles generated by the theoretical model of weak base diffusion (Equations 1-3 and Reactions 1 and 2). The $P^M_{NH_3}$ values used to calculate the theoretical curves are plotted in the *inset* as a function of the protein:lipid ratio. Buffer composition was as in Fig. 1.